Marchenko Multiple Elimination in a Resonant Pinch-Out Model

Slob, E.C.; Zhang, L.

DOI
10.3997/2214-4609.202011611

Publication date
2020

Document Version
Final published version

Published in
82nd EAGE Conference & Exhibition 2020

EAGE ANNUAL 2020
82ND CONFERENCE + EXHIBITION
AMSTERDAM | THE NETHERLANDS
NOW IN WINTER
8-11 DECEMBER

Fr_Dome5_02

Marchenko Multiple Elimination in a Resonant Pinch-Out Model

E. Slob[1]*, L. Zhang[1]

[1] Delft University of Technology

Summary

The ability to separate primary reflections from multiples is important for making subsurface images. Many existing methods need some form of model information and adaptive subtraction. Marchenko methods have been modified to operate at the acquisition surface. The associated filters can be computed from the reflection response without any model information. They are a function of a freely chosen time instant that defines the time window of the filter. The scheme can be implemented without adaptive subtraction. Applying the filter to the reflection response removes all multiples from the overburden that would arrive within the time window in which the filter is defined. For this reason, the first event in the result is a primary reflection event that can be taken and stored in a new dataset containing only primary reflections. From data of a resonant wedge model with thin layers, the images after MME show that destructive interference effects are removed by MME. Reflectors are imaged that are missing in the images of the reflection response. Thin layer effects cause incomplete prediction and removal of multiples. When MME treats the combined reflections from thin layers as a single complicated event, their combined multiples from other reflectors are properly removed.

Introduction

Multiples can be regarded a nuisance or a source of information. In either case, being able to discriminate multiples from primaries plays an important role in making better subsurface images. Multiples can be seen as helpful events that can fill in illumination gaps or improve the signal to noise ratio. Several studies aim to identify and use multiples in the imaging process (Whitmore et al., 2010; Verschuur and Berkhout, 2011; Zhang and Schuster, 2014; Wang et al., 2017; Davydenko and Verschuur, 2018). Multiples can be seen as repetitive combinations of primaries that carry only information that is present in the primaries. Several studies aim to predict and remove them from the data (Weglein et al., 1997; Jakubowicz, 1998; ten Kroode, 2002; Berkhout and Verschuur, 2005; Liu et al., 2018). Apart from ISS, these methods require some form of identification or model information and use adaptive subtraction.

A new family of methods has been introduced based on Marchenko inverse scattering (Wapenaar et al., 2013). A number of different approaches to data-driven redatuming and imaging without artefacts from multiples were derived and tested on synthetic and field data. Overburden removal (van der Neut and Wapenaar, 2016) led to Marchenko multiple elimination schemes. These schemes come with or without correction for transmission effects (Zhang and Staring, 2018; Zhang et al., 2019) and no model information or adaptive subtraction is necessary. The multiple elimination schemes use the reflection response to act as a filter on itself without needing other information than the source time signature. In principle the outcome is a dataset that contains primary reflections only, which forms ideal input for migration schemes that assume primary only data. As a byproduct the predicted multiples come as an additional dataset that can be used when desired to fill in illumination gaps or further improve signal to noise ratio or make up for a missing primary, or any other reason the user may have in mind. The methods can be seen as ways to separate primary reflections from multiples.

Independent of how a method predicts multiples, all multiples are assumed to not overlap with the associated primary reflections. When two consecutive primary reflections, e.g., from the top and bottom of a layer, overlap, that layer can be said to be thin. The first interbed multiple will overlap with the primary from the bottom. When the layer becomes even thinner, more overlap will ultimately lead to the inability to distinguish between two (or more) primary reflections and interbed multiples. At some point, model-driven, data-driven or hybrid methods will all fail in the sense that multiples will not be predicted anymore and two overlapping primary reflections will be treated as a single primary with a more complicated time behaviour. A simple single thin layer example was given and analysed in Slob et al. (2014). Verschuur (2019) presented an interesting thin layer example using a pinching out wedge model bounded in top and bottom by two horizontal reflectors. Here we investigate the performance of the Marchenko multiple elimination (MME) scheme on a similar but resonant model and look at the effect of two different centre frequencies of the source time function on the ability of the scheme to separate primary reflections from multiples and use the primaries to compute migration images.

Brief review of Marchenko Multiple Elimination

In Marchenko redatuming, the receivers at the acquisition surface are redatumed to a chosen position inside the heterogeneous medium (Wapenaar et al., 2014a). This chosen position becomes a virtual receiver point and the resulting field at that receiver is the corresponding virtual impulse response or Green's function with the sources unchanged in their original location. The up- and down-going parts of this Green's function are used to create images without artefacts of multiple reflections, which has become known as Marchenko imaging (Wapenaar et al., 2014b). The redatuming step requires knowledge of the first arrival of the field from the sources to the virtual receiver. This estimate is used to compute the initial part of the down-going focusing function. The required knowledge can be built, e.g., with a macro-velocity model. Once this estimate is known the Green's functions and the artefact-free subsurface image are obtained without requiring further model information.

The need to know the initial part of the down-going focusing function was removed in van der Neut and Wapenaar (2016) to remove the effect of the overburden. This is done by projecting the initial down-going parts of all focusing functions at a certain depth level back to one physical receiver at the acquisition surface. This projection has two merits. The first is that the initial down-going part of the projected focusing function has become a unit impulse in the horizontal position of the physical receiver and in time. It is no longer an unknown. The second is that the timing of all events in the resulting up-going part of projected Green's function is the same as that of the data. The time truncations are now a function of some two-way travel time from a source to the former focusing level and back to the receiver. This would require model information to accommodate the offset dependent travel times.

The need for model information was removed in Zhang and Staring (2018) who showed that offset independent time truncations can be used. The truncation time is now a free parameter that can be chosen as any desired output time of the scheme. At this point the Marchenko multiple elimination scheme is totally model free. The primary reflections that are filtered out from the reflection response can be collected in a new dataset, where they occur at their physical two-way travel time and with their physical amplitude including transmission effects. This means that the primary reflections are filtered out from the projected Green's functions. This is the Marchenko multiple elimination (MME) scheme.

The up- and down-going parts of the filter are wave fields computed from the reflection response as

$$h^-(\mathbf{x}_0',\mathbf{x}_0'',t,\tau) - \int_{\partial\mathbb{D}_0} R(\mathbf{x}_0',\mathbf{x},t) * h^+(\mathbf{x},\mathbf{x}_0'',t,\tau)\mathrm{d}\mathbf{x} = R(\mathbf{x}_0',\mathbf{x}_0'',t), \quad (1)$$

$$h^+(\mathbf{x}_0',\mathbf{x}_0'',t,\tau) - \int_{\partial\mathbb{D}_0} R(\mathbf{x}_0',\mathbf{x},-t) * h^-(\mathbf{x},\mathbf{x}_0'',t,\tau)\mathrm{d}\mathbf{x} = 0. \quad (2)$$

In these equations the up- and down-going parts of the filter are denoted $h^\pm(\mathbf{x}_0',\mathbf{x}_0'',t,\tau)$ where the plus- and minus-signs indicate down- and up-going parts, respectively, t is time and τ is truncation time and $*$ indicates temporal convolution. The position vectors denote the receiver and source locations $\mathbf{x}_0',\mathbf{x}_0''$, respectively, in the reflection response and $\mathbf{x}$ is the coordinate vector for all sources at the acquisition surface $\partial\mathbb{D}_0$. Once h^+ is known, we retrieve the time sample for the primary reflection dataset R_t as

$$R_t(\mathbf{x}_0',\mathbf{x}_0'',\tau+\varepsilon) = R(\mathbf{x}_0',\mathbf{x}_0'',\tau+\varepsilon) + \int_{\partial\mathbb{D}_0} R(\mathbf{x}_0',\mathbf{x},t) * h^+(\mathbf{x},\mathbf{x}_0'',t,\tau)\mathrm{d}\mathbf{x}, \quad (3)$$

where ε is half the time-duration of the source time signature.

Example of resolution problem and interference effects

We use a constant velocity of 2000 m/s and two density values of 1000 kg/m^3 and 2000 kg/m^3, resulting in local reflection coefficients of $r = \pm 1/3$ in the model. The model is an embedded wedge between two horizontal reflectors. The wedge has six layers with alternating density, a thickness of 100 m in the left side of the model, which vanish in the right side of the model. We use a 15 Hz and a 30 Hz Ricker wavelet to model the data with 401 sources and receivers spaced at 10 m. All wedge layers have the same thickness in our model, contrary to the model in Verschuur (2019), resulting in a resonant model. One-way wave equation migration with the correct velocity is used for creating the images.

Figure 1 shows the resulting images overlaying the density model. The grey and yellow colours in the background indicate 1000 kg/m^3 and 2000kg/m^3. The top and bottom rows show images of the reflection response before and after MME. The left and right columns show result with 15Hz and 30 Hz Ricker wavelets. We discuss three interesting features that can be seen in the model results. The first is that in the images in the top row we can see that the reflections from first three layers in the wedge do not suffer from interference and are properly imaged up to the location that corresponds approximately to a thickness that is half the wavelength at the centre frequencies. The reflectors can still be identified as separate reflectors up to a layer thickness approximately equal to 35% of the wavelength at the centre frequency. After that the overlap is so large that the interpretation becomes ambiguous. These are the first four dipping reflectors. The fifth reflector is quite weak where it shows up as an individual reflector with the 15 Hz wavelet, whereas its presence with the 30Hz wavelet is clearer due to the improved resolution, even though there it also becomes weaker towards the left side of the model. The second is that the top and bottom of the last dipping layer that pinches out toward the right are not clearly present in

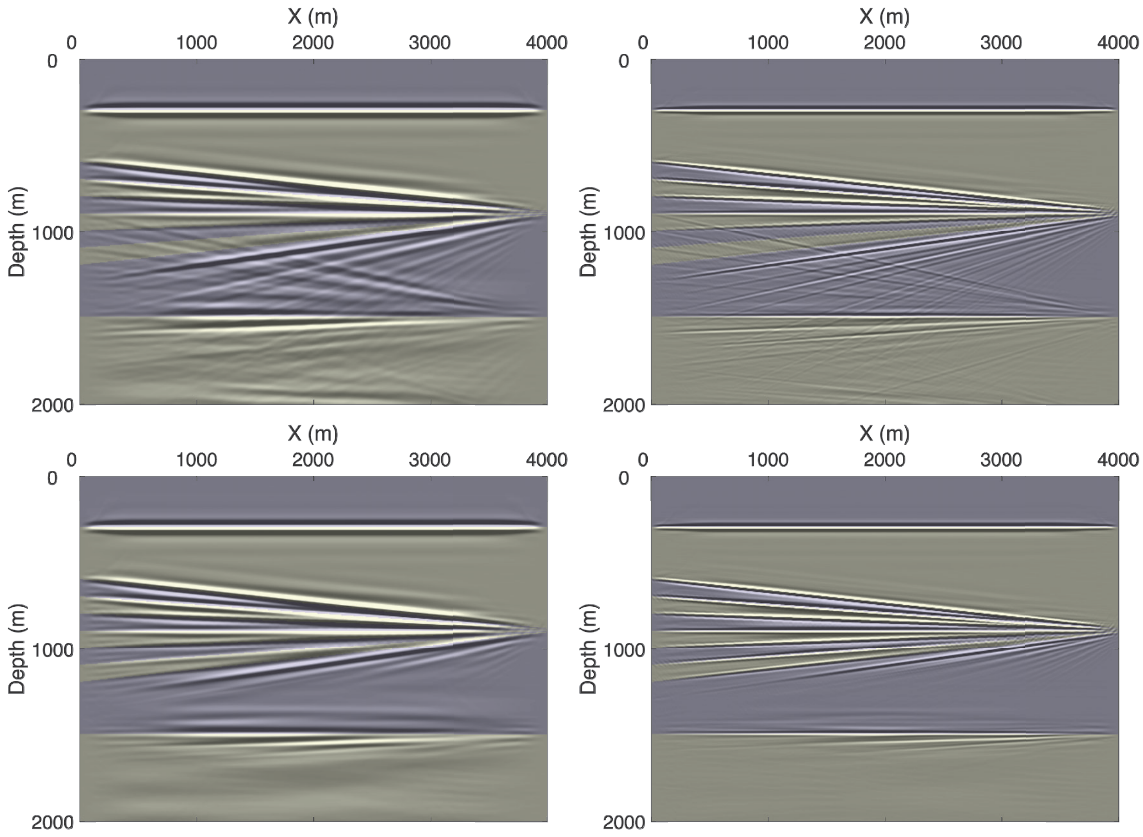

Figure 1 *Images overlaying the density model: grey and yellow colours in the background represent 1000 kg/m*^{3} *and 2000kg/m*^{3}*. The top row show images of the reflection response before and the bottom row after MME. Left column shows 15 Hz and right column shows 30 Hz Ricker wavelet results.*

either image. Instead a strong event can be seen that could be easily interpreted as a reflector. The third is that the dipping layers pinching out have a strong imprint on the imaged bottom horizontal reflector.

The MME scheme does not do much to improve the image where the effects are due to thin layering alone. This can be seen in the right most km of the image and the presence of the multiples in that part of the model after MME. MME restores the bottom two missing dipping reflectors and improves the visibility of the fifth dipping reflector. This is true for both wavelets. MME reduces the presence of multiples in the first 3 km of the model as can be seen in the reduction of multiples between the deepest dipping reflector and the bottom horizontal reflector. The presence of the layers in the wedge is visible in the imaged bottom horizontal reflector with the 15 Hz wavelet, whereas that presence is reduced with the 30 Hz wavelet. Notice that the multiples that show up as a mirror image copy of the layers in the wedge around the bottom horizontal reflector are almost perfectly removed in the entire model.

Full wave field migration requires a velocity model to make updates in the reflection operator at every depth level. These updates are obtained through an inversion procedure by iterative forward modelling (Davydenko and Verschuur, 2017). If the scheme is implemented with adaptive subtraction it will be difficult to recover the missing primaries such as from the bottom two dipping reflectors that were recovered and properly imaged by MME in this example. It will be interesting to compare outcomes of such limitation studies and the associated computational cost to obtain results with the two methods.

Conclusions

We have shown that with MME reflectors are imaged that are missing in images from the original data. MME recovers primaries that are missing in the data due to interference effects. Schemes that require adaptive subtraction will not likely recover these. Resolution limitations were shown to prevent the

MME scheme to predict associated multiples when the layers become too thin. When the layers become so thin that the whole pack of layers are treated as one layer, their multiple reflections from boundaries of sufficiently thick layers are still almost completely removed. This seems to suggest that these heavily convoluted reflections are treated as a single more complicated primary reflection by the MME scheme.

Acknowledgements

The authors thank Eric Verschuur for sharing model information and Delphi Consortium for its support.

References

Agranovich, Z.S. and Marchenko, V.A. [1963] *The inverse problem of scattering theory*. Gordon and Breach, New York.

Berkhout, A.J. and Verschuur, D.J. [2005] Removal of internal multiples with the common focus-point (CFP) approach. Part 1: Explanation of the theory. *Geophysics*, **70**(3), V45–V60.

Davydenko, M. and Verschuur, D.J. [2017] Full-wavefield migration: using surface and internal multiples in imaging. *Geophysical Prospecting*, **65**(1), 7–21.

Davydenko, M. and Verschuur, D.J. [2018] Including and using internal multiples in closed-loop imaging - Field data examples. *Geophysics*, **83**(4), R297–R305.

Jakubowicz, H. [1998] Wave equation prediction and removal of interbed multiples. In: *SEG Technical Program Expanded Abstracts*. 1527–1530.

ten Kroode, F. [2002] Prediction of internal multiples. *Wave Motion*, **35**(4), 315–338.

Kunetz, G. [1964] Generalisation des operateurs d'anti-resonance a un nombre quelconque de reflecteurs. *Geophysical Prospecting*, **12**(3), 283–289.

Liu, J.H., Hu, T.Y. and Peng, G.X. [2018] Suppressing seismic inter-bed multiples with the adaptive virtual events method. *Chinese Journal of Geophysics-Chinese Edition*, **61**(3), 1196–1210.

van der Neut, J. and Wapenaar, K. [2016] Adaptive overburden elimination with the multidimensional Marchenko equation. *Geophysics*, **81**(5), T265–T284.

Slob, E., Wapenaar, K., Broggini, F. and Snieder, R. [2014] Seismic reflector imaging using internal multiples with Marchenko-type equations. *Geophysics*, **79**(2), S63–S76.

Verschuur, D.J. and Berkhout, A.J. [2011] Seismic migration of blended shot records with surface-related multiple scattering. *Geophysics*, **76**(1), A7–A13.

Verschuur, E. [2019] Imaging including internal multiples: Influence of broadband acquisition. In: *Extended Abstracts of the 81st EAGE Conference and Exhibition 2019*. WS08–14.

Wang, Y., Y.Zheng, Xue, Q., Chang, X., Fei, T.W. and Luo, Y. [2017] Reverse time migration of multiples: Reducing migration artifacts using the wavefield decomposition imaging condition. *Geophyiscs*, **82**(4), S307–S314.

Wapenaar, K., Broggini, F., Slob, E. and Snieder, R. [2013] Three-Dimensional Single-Sided Marchenko Inverse Scattering, Data-Driven Focusing, Green's Function Retrieval, and their Mutual Relations. *Physical Review Letters*, **110**(8), 084301.

Wapenaar, K., Thorbecke, J., van der Neut, J., Broggini, F., Slob, E. and Snieder, R. [2014a] Green's function retrieval from reflection data, in absence of a receiver at the virtual source position. *Journal of the Acoustical Society of America*, **135**(5), 2847–2861.

Wapenaar, K., Thorbecke, J., van der Neut, J., Broggini, F., Slob, E. and Snieder, R. [2014b] Marchenko Imaging. *Geophysics*, **79**(3), WA39–WA57.

Weglein, A.B., Gasparotto, F.A., Carvalho, P.M. and Stolt, R.H. [1997] An inverse scattering series method for attenuating multiples in seismic reflection data. *Geophysics*, **62**, 1975–1989.

Whitmore, N.D., Valenciano, A.A. and Sollner, W. [2010] Imaging of primaries and multiples using a dual-sensor towed streamer. In: *SEG Technical Program Expanded Abstracts*. 3187–3192.

Zhang, D. and Schuster, G.T. [2014] Least-squares reverse time migration of multiples. *Geophysics*, **79**(1), S11–S21.

Zhang, L. and Staring, M. [2018] Marchenko scheme based internal multiple reflection elimination in acoustic wavefield. *Journal of Applied Geophysics*, **159**, 429–433.

Zhang, L., Thorbecke, J., Wapenaar, K. and Slob, E. [2019] Transmission compensated primary reflection retrieval in the data domain and consequences for imaging. *Geophysics*, **84**(4), Q27–Q36.